Signal Types Investigation for Harmonic Modulation in Drives

Peter Häuptle, *Member, IAENG,* Peter Hubinský, Boris Rudolf and Gerhard Gruhler

***Abstract*—In this contribution we focus on a method which is able to reduce an unwanted oscillation in a mechatronic drive system. A mechatronic drive consists of a motor, a gear-box, electronics and control joint to one module. When now applying the method of harmonic modulation, i.e. the modulation of the set-point signal used within the mechatronic drive, oscillations of the system (at e.g. the end-effector) can be reduced. A single sine-signal was commonly used for modulation. In the following we want to discuss and investigate other signal-types as well as presenting their results.**

***Index Terms*—oscillation, control, harmonic-modulator, feed-forward, mechatronic**

I. Introduction

An undesirable oscillation often occurs in mechatronic systems (MS) due to a relatively low damped system behavior. Especially in lightweight applications or robotics where position accuracy is a manner, the performance basically can only be held by the cost of speed, power or mechanical construction efforts. Hence, improvement in control might be an additional and smart way. Two different types of oscillations, namely the "transient" as well as the "semi-steady-state" oscillations are known [1, 2]. Good results in feedback and state-space control methods have been made by [3, 4, 5, et al.] by the cost of additional sensors or relatively huge calculation efforts. For eliminating transient oscillations good results have been made by [6, 7, 8, 9, et al.] due to feed-forward based methods. A further feedforward method is the already mentioned harmonic modulation, where especially semi-steady-state oscillations can be reduced [10]. Before we are able to start with the investigation to other signal-types, lets introduce the mechatronic system used here.

A. Mechatronic system

Based on an experimental setup, the main modeling results can be concentrated in Table. I and Equ. 1 [1, 2]. Here, the MS is interpreted as a low damped *P-T*$_2$ system; a torsional damped spring mass in detail.

Where i indicates the gear-ratio, c the torsional spring constant, d the damping constant and J_{all} the overall moment of inertia. The resonance frequency $f_r = f_0 \cdot \sqrt{1-2\cdot D^2}$, the eigen frequency f_0 and the damped oscillating frequency f_d are also shown in Table. I [1, 2].

Manuscript received June 30, 2011; revised August 18, 2011. This work was supported in part by the company SCHUNK GmbH & Co. KG in Lauffen Germany.

P. Häuptle, P. Hubinský and B. Rudolf are with the Faculty of Electrical Engineering and Information Technology, Slovak University of Technology, Bratislava SK, 812-19 EU e-mail: peter.haeuptle@web.de, {peter.hubinsky, boris.rudolf}@stuba.sk.

G. Gruhler is with the Faculty of Mechanics and Electronics, Heilbronn University, Heilbronn D, 74081 EU e-mail: gruhler@hs-heilbronn.de

TABLE I
System parameters. [1, 2]

PARAMETER:	VALUE:	UNIT:
i	1/121	-
c	2409	Nm/rad
d	0.54	Ns/m
J_{all}	0.2132134	kg m^2
D	0.012	-
f_r	16.917	Hz
f_0	16.919	Hz
f_d	16.918	Hz

$$G_{(s)} = \frac{i}{1 + 2\cdot D\cdot \frac{s}{\omega_0} + \frac{s^2}{\omega_0^2}}$$
$$D = \frac{d}{2\cdot c\cdot \sqrt{\frac{J_{all}}{c}}} \quad < 1 \tag{1}$$

B. The harmonic modulation

Let's further consider a trapezoidal (velocity) set-point generation where it's often used for mechatronic drives (MD) like shown *(dashed)* in Fig. 1). The harmonic modulated version will then last in the *(solid)* line.

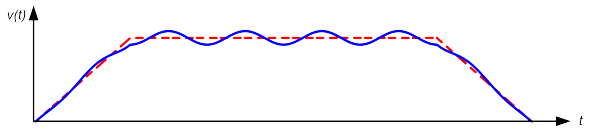

Fig. 1. Standard trapez *(dashed)* vs. harmonic modulated trapez *(solid)*.

C. Bode simulation technique

The inverse Laplace transform of the system transfer function Equ. 1 is *g(t)*. Then, bode can be obtained using Equ. 2 [10]:

$$\left[\mathcal{L}\left\{g(t)\right\} + K_h\cdot\mathcal{L}\left\{y(t)\cdot g(t)\right\}\right]_{(s\to j\omega)} = G_{all\,(j\omega)} \tag{2}$$

The gain of modulation is K_h and the modulation frequency is f_{mod} like stated out in Equ. 3 [10]:

$$K_h = K_{perc.}\cdot(\dot{\varphi}_M\cdot i)$$
$$K_h = K_{perc.}\cdot(\omega_M\cdot i) \tag{3}$$
$$\tilde{\omega} = 2\pi f_{mod}$$

ISBN: 978-988-19251-7-6
ISSN: 2078-0958 (Print); ISSN: 2078-0966 (Online)

In case of using a single sine-signal (see add. Equ. 8, Fig. 2 and Fig. 3) it lasts to Equ. 4 [10]:

$$G_{all(j\omega)} = G(j\omega) + K_h \cdot \frac{1}{j2} \cdot [G(j\omega - j\tilde{\omega}) - G(j\omega + j\tilde{\omega})] \quad (4)$$
$$where \quad y(t) = \sin(\tilde{\omega}t)$$

In case of a cosine signal to Equ. 5 respectively.

$$G_{all(j\omega)} = G(j\omega) + K_h \cdot \frac{1}{2} \cdot [G(j\omega - j\tilde{\omega}) + G(j\omega + j\tilde{\omega})] \quad (5)$$
$$where \quad y(t) = \cos(\tilde{\omega}t)$$

II. Problem Statement

The technique of harmonic modulation with a single sine-wave-signal is maybe improvable when using different signal-types or e.g. a multiple of sine-signals. Simulation results as well as real measured results with the single sine-signal have been made here [10]. Basically the modulation which can be seen as frequency shifting (MD velocity shifting) avoids staying constantly in the resonance zone, although in mean the specific set-point is held. *(Note: The mean of periodic signal without a DC-offset is zero.)* So the reduction of an unwanted oscillation is made by the cost of a "slightly swinging" set-point signal (solid, in Fig. 1) around the previous set-point (dashed, in Fig. 1)

III. Signal-types

First of all, let's consider a time periodic signal whose fundamental angular frequency can be stated out to:

$$\omega = 2\pi f = \frac{2\pi}{T} \quad (6)$$
$$i.e. \quad \omega = 2\pi \cdot 0.4\,Hz$$

Then, due to Fourier, we can break such a signal to a series of sine- and cosine-signals in the form of:

$$y_{(t)} = \frac{a_0}{2} + \sum_{n=1}^{\infty} [a_n \cdot cos(n \cdot \omega \cdot t) + b_n \cdot sin(n \cdot \omega \cdot t)] \quad (7)$$

Where $a_0 = 0$ when no DC-offset is present in the signal. Having the so named fourier-coefficients (a_n and b_n) any periodic signal can be build up. In the following several (common) signal types will be introduced. On the left hand side of each figure, the signal by time is plotted. On the right hand side the respectively (normed) histogram of residence is plotted. Further each interpretation in sense of fourier-series is shown as well. Note: We only seek for AC-signals without any offset.

A. Basic types

1) Sine-signal: Let's start with the trivial case, where the fundamental frequency itself is the signal i.e. the sine-signal:

$$y_{(t)} = sin(n \cdot \omega \cdot t) \quad ; \quad where\ n = 1 \quad (8)$$

The maximum and minimum values of Fig. 2 are also the values with the longest residence like shown in Fig. 3. Good fitting results using this signal for harmonic modulation have been made in [10]. As already mentioned the histogram in Fig. 3 shows that in sense of avoiding the resonance zone of we stay mainly above and below equally. A further advantage is that no higher harmonics ($n > 1$ in Equ. 8) is contained in the signal and therefore no additional concern in coinciding with the system resonance frequency f_r is existing.

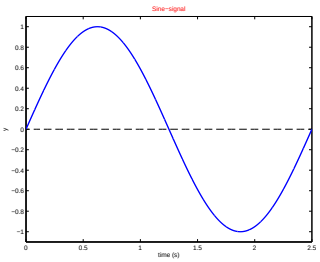

Fig. 2. Sine-signal

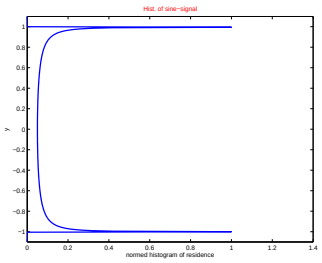

Fig. 3. Hist. of sine-signal

2) Triangle-signal: A signal where the arrangement in the histogram of residence is constant (see add. App. B) is also known the triangle-signal (see Fig. 4 and 5).:

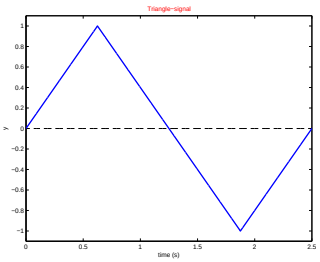

Fig. 4. Triangle-signal

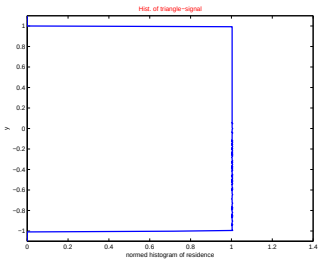

Fig. 5. Hist. of triangle-signal

$$y_{(t)} = \frac{8}{\pi^2} \sum_{n=1,3,5,\ldots}^{\infty} \frac{(-1)^{(\frac{n-1}{2})}}{n} \cdot sin(n \cdot \omega \cdot t) \quad (9)$$

We can see that higher harmonics ($n > 1$ in Equ. 9) are existing. These higher frequency content is less compared to the "pure" square-wave. Higher harmonics are able to cause other resonance effects, but when also having transient phases it could be better having a uniformly distributed histogram [11] (see also Fig. 9).

3) Square-wave-signal: The signal with the best avoidance of the resonance zone might be the square-wave-signal (see Fig. 6 and 7).:

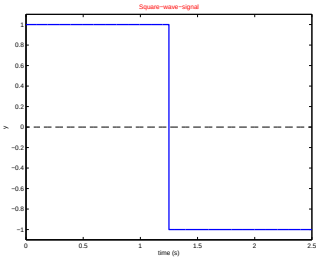

Fig. 6. Square-wave-signal

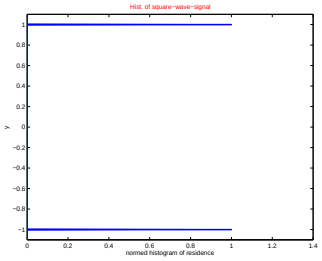

Fig. 7. Hist. of sq.-wave-signal

$$y_{(t)} = \frac{4}{\pi} \sum_{n=1,3,5,\ldots}^{\infty} \frac{1}{n} \cdot sin(n \cdot \omega \cdot t) \quad (10)$$

Higher harmonics ($n > 1$ in Equ. 10) are existing which are able to cause transient-effects when coinciding with f_r. But the implementation of the square-wave-signal (see add. Equ. 10) offers four opportunities: *If no or little system information is known ($\approx f_0$, $\approx f_d$, $\approx f_r$):*

- The ideal square-wave with ($n = 1, 3, 5, \ldots\infty$).

ISBN: 978-988-19251-7-6
ISSN: 2078-0958 (Print); ISSN: 2078-0966 (Online)

- The approximated order square-wave with $(n = 1, 3)$ *2nd order* or $(n = 1, 3, 5)$ *3rd order*.

If detailed system information is known (f_0, f_d, f_r):

- The filtered square-wave with e.g. *notch-* or *band-elimination*-filters $(n = 1, 3, 5, ...\infty \ni n \cdot \omega \cong \omega_r)$.
- The shaped square-wave with e.g. *ZV-*, *ZVD-*, *ZVD^x*-shaper [6] or *posicast* [7] (at i.e. f_d)

4) Pulse-signal: Further, when i.e. ω_r is known. We are able to improve the avoidance of the resonance zone when not using a cyclic duration where positive- and negative-values are equally disposed. (This can be seen as a duty cycle different to a ratio of "1:1". See add. Fig. 7 and 9). Such a periodic signal without any offset is e.g. the pulse-signal shown in Fig. 8.:

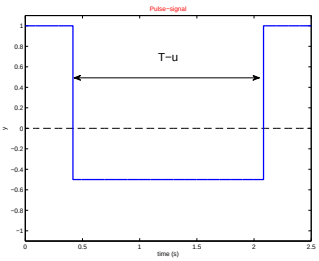

Fig. 8. Pulse-signal

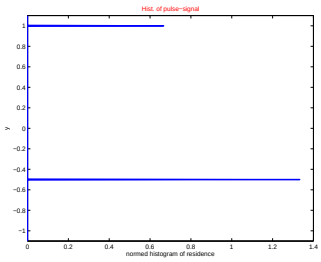

Fig. 9. Hist. of pulse-signal

Note: Here u was one third of T. In case when u is exactly the half of T, it lasts to a square-wave-signal.

$$y_{(t)} = \frac{4}{\pi} \sum_{n=1}^{\infty} \frac{1}{n} \cdot sin\left(\frac{u \cdot n \cdot \omega}{2}\right) \cdot cos(n \cdot \omega \cdot t) \qquad (11)$$
$$where: \quad 0 < u < T$$

Here, beside adjusting u also approx. and/or filtering can be applied like introduced at the square-wave-signal before. The further advantage compared to the square-wave-signal is, when a working point were an unwanted oscillation is not on the top of the resonance zone ($\omega = \omega_d$) but already in the resonance zone. This is for instance the case, when either the top or the bottom of the most history of residence (Fig. 7) is matching ω_d, then a histogram of residence like shown in Fig. 9 may last in a better behavior. Then, compared to the square-wave-signal (where it's equal above and below dispersed see Fig. 7) it might be better to have an avoidance where it's better staying more above than below (when $\omega > \omega_d$ and $0 < u < T/2$) or inversely staying more below than above (when $\omega < \omega_d$ and $T/2 < u < T$) that point (see Fig. 9).

B. Approximated types

Instead of using a huge order $(n = 1...\infty)$ in sense of Fourier series, we reduced the order to: $(n = 1, 3)$ *2nd order* or $(n = 1, 3, 5)$ *3rd order* like shown in Fig. 10 to 13.

For the pulse-signal we used the order $(n = 1, 2)$ *2nd order* and $(n = 1, 2, 3)$ *3rd order* like shown in Fig. 14 to 17.

The dashed-dotted, line in Fig. 18 should additionally indicate the *pure* triangle-signal.

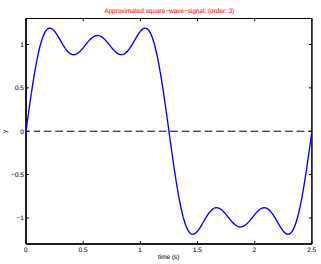

Fig. 10. 3rd order sq.-w.-signal

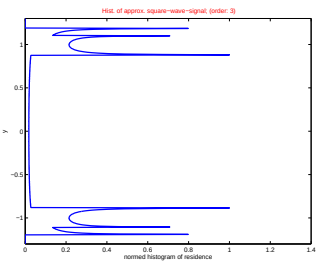

Fig. 11. Hist. of 3rd o. sq.-w.

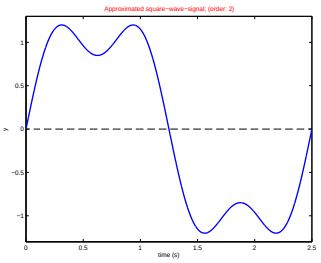

Fig. 12. 2nd order sq.-w.-signal

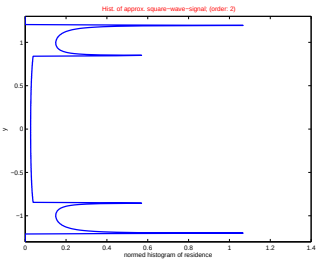

Fig. 13. Hist. of 2nd o. sq.-w.

IV. Results

To make the results visible, several bode plots were discussed in the following. *Note: The bode plots are plotted linear instead of logarithmic. The DC-gain of the system transfer function (Equ. 1) is set to one instead to the gear-ratio.* The *(dashed)* line shows the bode of the normal system transfer function (Equ. 1); the *(dashed dotted)* line shows the bode of just the harmonic modulator transfer function and the *(solid)* line shows the bode of the complete system transfer function (Equ. 2). As long as the solid blue line is "below" the dashed magenta line in the resonance zone, there is an improvement in sense of reducing an unwanted oscillation. In Fig. 21 the single sine-signal (like introduced in Fig. 2 and it's Hist. in Fig. 3, which itself has an analytical interpretation formulated in Equ. 8,) was applied in [10]:

The approx. square-wave-signals (see add. Equ. 10) are shown in Fig. 22 (3rd order see add. Fig. 10 and 11) as well as Fig. 23 (2nd order see add. Fig. 12 and 13):

The approx. pulse-signals (see add. Equ. 11) are shown in Fig. 24 (3rd order see add. Fig. 16 and 17) as well as Fig. 25 (2nd order see add. Fig. 14 and 15):

To compare the results, Fig. 22 to 25 should always be related to Fig. 21. Further tests with other signal-types e.g. sawtooth etc. didn't show great promise.

V. Conclusion

The use of higher order modulation signals (to obtain a more square-wave-signal) allows a less modulation gain (i.e. from 8 to 5per.) by same or slightly better performances in sense of reducing an unwanted oscillation. This might also be depending on the system damping *(d)*. The use of an approximated pulse-signal can additionally improve the performance at the "lower gain" of the resonance zone (between 8-15Hz and ca. 18-20Hz). A varying *u* (e.g. $T/2-x < u < T/2+x$) around f_d can led to an even better performance by the cost of finding a good fitting relation of *u* (Let *u* be a function of f_d and *T*). It is very important that the use of any higher order signal will force the user to take care of not coinciding

ISBN: 978-988-19251-7-6
ISSN: 2078-0958 (Print); ISSN: 2078-0966 (Online)

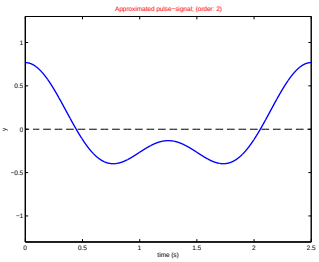

Fig. 14. 2nd order pulse-signal

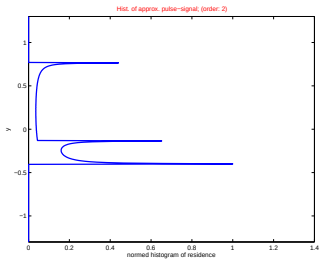

Fig. 15. Hist. of 2nd o. pulse

the modulation frequency content with the system resonance frequency/ies.

APPENDIX A
ANALYTICAL HIST.-FUNCTION OF SINE-SIGNAL

The solution of the histogram from a single sine signal can be found in [12, 13].

$$hist_{y\,(\gamma)} = \frac{1}{\pi} \cdot \frac{1}{\sqrt{1-y^2}}$$
$$where: \tag{12}$$
$$y_{(t)} = sin(\omega \cdot t)\ ;\ -\frac{T}{4} < t \leq \frac{T}{4}$$

where T is one period of the signal.

APPENDIX B
ANALYTICAL HIST.-FUNCTION OF TRIANGLE-SIGNAL

In [11]:

$$hist_{y\,(\gamma)} = \frac{1}{c_{max}} = \frac{1}{1+a}$$
$$for\ ;\ -\frac{T}{4} < t < \frac{T}{4} \tag{13}$$

where, c_{max} is the maximum amplitude value of the triangle-signal.

APPENDIX C
ANALYTICAL HIST.-FUNCTION OF APPROX. TRIANGLE-SIGNAL

The solution of the histogram from an approximated triangle signal (2nd order) was already introduced in [11].

$$hist_{c\,(\gamma)} = \frac{\overline{x}}{\alpha \cdot \sqrt{1-x^2} \cdot 12 \cdot \pi \cdot a}$$
$$for:\ \ 0 < a \leq \frac{1}{3}\ \ ;\ \ 0 \leq t \leq \frac{T}{4}$$
$$where:$$
$$\alpha = \sqrt{\left(\frac{\gamma}{8 \cdot a}\right)^2 \cdot \left(\frac{1-3 \cdot a}{12 \cdot a}\right)^3} \tag{14}$$
$$\overline{x} = \sqrt[3]{\alpha + \left(\frac{\gamma}{8 \cdot a}\right)} + \sqrt[3]{\alpha - \left(\frac{\gamma}{8 \cdot a}\right)}$$
$$x = \sqrt[3]{\alpha + \left(\frac{\gamma}{8 \cdot a}\right)} - \sqrt[3]{\alpha - \left(\frac{\gamma}{8 \cdot a}\right)}$$

where $a = \frac{1}{c_{max}} - 1$.

ACKNOWLEDGMENT

The authors would like to thank Mr. & Ms. Schunk as well as the R&D group of the company SCHUNK GmbH.

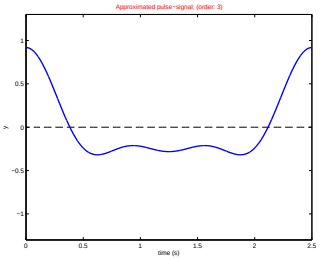

Fig. 16. 3rd order pulse-signal

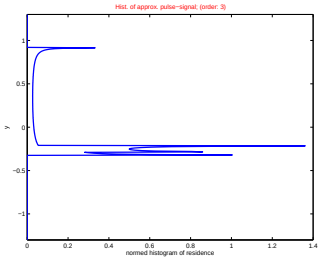

Fig. 17. Hist. of 3rd o. pulse

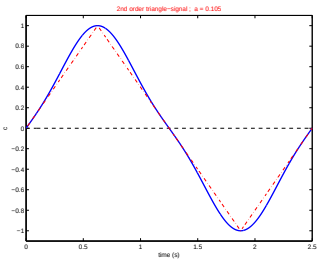

Fig. 18. 2nd order triangle-signal [11]

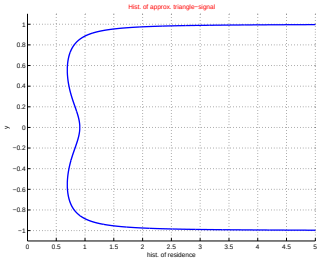

Fig. 19. Hist. of 2nd order triangle-signal [11]

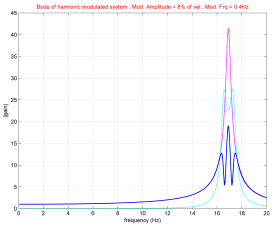

Fig. 20. Bode: Single sine *(8% vel & 0.4Hz)* [10]

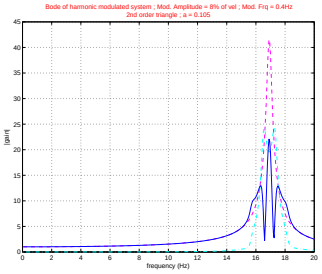

Fig. 21. Bode: Triangle 2nd *(8% vel & 0.4Hz)* [11]

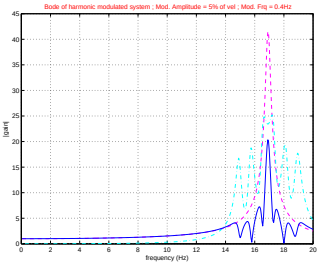

Fig. 22. Bode: Square-wave 3rd *(5% vel & 0.4Hz)*

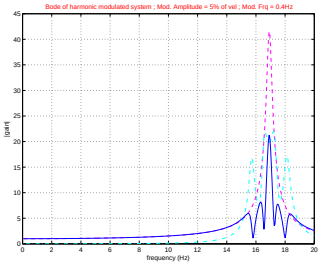

Fig. 23. Bode: Square-wave 2nd *(5% vel & 0.4Hz)*

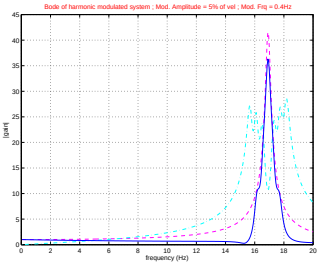

Fig. 24. Bode: Pulse 3rd *(5% vel & 0.4Hz)*

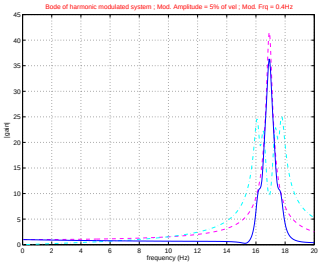

Fig. 25. Bode: Pulse 2nd *(5% vel & 0.4Hz)*

ISBN: 978-988-19251-7-6
ISSN: 2078-0958 (Print); ISSN: 2078-0966 (Online)

REFERENCES

[1] P. Häuptle, P. Hubinský, G. Gruhler, and B. Fellhauer, *Modellierung des Schwingungsverhaltens eines Mechatronischen Antriebes hinsichtlich dem Entwurf verschiedener Regelungstechniken - Internationales Forum für Mechatronik*. IFM-ZHAW - Institut für Mechatronische Systeme, Winterthur, Swiss, Nov. 2010.

[2] P. Häuptle, G. Gruhler, and P. Hubinský, *Frequency Domain Identification of a Mechatronic System*. Proc. of the Hefei-Heilbronn Workshop on Research in Education in Mechatronics, Heilbronn, Germany, Jun. 2010.

[3] P. Gandhi and F. Ghorbel, "Closed-loop compensation of kinematic error in harmonic drives for precision control applications," *Control Systems Technology, IEEE Transactions on*, vol. 10, no. 6, pp. 759–768, 2002.

[4] H. Taghirad, "Robust torque control of harmonic drive systems," Ph.D. dissertation, Citeseer, 1997.

[5] T. Tuttle and W. Seering, "A nonlinear model of a harmonic drive gear transmission," *Robotics and Automation, IEEE Transactions on*, vol. 12, no. 3, pp. 368–374, 1996.

[6] W. Singhose, "Command shaping for flexible systems: A review of the first 50 years," *International Journal of Precision Engineering and Manufacturing*, vol. 10, no. 4, pp. 153–168, 2009.

[7] O. Smith, "Posicast control of damped oscillatory systems," *Proceedings of the IRE*, vol. 45, no. 9, pp. 1249–1255, 1957.

[8] T. Pospiech and P. Hubinský, "Slosh-free positioning of containers with liquids and flexible conveyor belt," *JEEEC*, vol. 61, no. 2, 2010.

[9] P. Häuptle and P. Hubinský, "Embedded shaping technique to reduce oscillations in intelligent drives," in *Proc. of the 6th South East European Doctoral Student Conference in Thessaloniki, Greece*.

[10] P. Häuptle, P. Hubinský, and G. Gruhler, "Harmonic modulation in control to reduce oscillations in mechatronic systems," in *Proc. of the INES in Poprad, Slovakia*. IEEE, Jun. 2011, pp. 303–308.

[11] P. Hubinský, B. Rudolf, and P. Häuptle, "Selected topics in modelling and control. vol. 7. - optimization of the signal-type used in a harmonic modulator for control."

[12] H. Levitan, J. Segundo, G. Moore, and D. Perkel, "Statistical analysis of membrane potential fluctuations:: Relation with presynaptic spike train," *Biophysical journal*, vol. 8, no. 11, pp. 1256–1274, 1968.

[13] A. Papoulis, S. Pillai, and S. Unnikrishna, *Probability, random variables, and stochastic processes*. McGraw-hill New York, 1965, vol. 196.

ISBN: 978-988-19251-7-6
ISSN: 2078-0958 (Print); ISSN: 2078-0966 (Online)